European-Scale Drought: Understanding Connections between Atmospheric Circulation and Meteorological Drought Indices

DANIEL G. KINGSTON

Department of Geography, University of Otago, Dunedin, New Zealand

JAMES H. STAGGE AND LENA M. TALLAKSEN

Department of Geosciences, University of Oslo, Oslo, Norway

DAVID M. HANNAH

School of Geography, Earth and Environmental Sciences, University of Birmingham, Birmingham, United Kingdom

(Manuscript received 18 December 2013, in final form 9 October 2014)

ABSTRACT

Quantification of large-scale climate drivers of drought is necessary to understand better and manage these spatially extensive and often prolonged natural hazards. Here, this issue is advanced at the continental scale for Europe. Drought events are identified using two indices—the 6-month cumulative standardized precipitation and standardized precipitation evapotranspiration indices (SPI-6 and SPEI-6, respectively)—both calculated using the gridded Water and Global Change (WATCH) Forcing Dataset for 1958–2001. Correlation of monthly time series of the percentage of European area in drought with geopotential height for 1958–2001 indicates that a weakening of the prevailing westerly circulation is associated with drought onset. Such conditions are linked to variations in the eastern Atlantic/western Russia (EA/WR) and North Atlantic Oscillation (NAO) atmospheric circulation patterns. Event-based analysis of the most widespread European droughts reveals that a higher number are identified by the SPEI-6 than the SPI-6, with SPEI-6 drought events showing a greater variety of spatial locations and start dates. Atmospheric circulation drivers also vary between the two types of events, with EA/WR-type variation associated most frequently with SPEI-6 drought, and the NAO associated with SPI-6. This distinction reflects the sensitivity of these drought indices to the underlying drought type (meteorological water balance versus precipitation, respectively) and associated differences in their timing and location (Europe-wide year round versus northern Europe winter). As such, this study provides new insight into both the identification of Europe-wide drought and patterns of large-scale climate variation associated with two different drought indices.

1. Introduction

Droughts are a recurrent natural hazard, characterized by below natural water availability (Tallaksen and van Lanen 2004) with widespread environmental and societal consequences (e.g., Ji and Peters 2003; Monk et al. 2008; Tsakiris et al. 2010; Vicente-Serrano et al. 2012; Haslinger et al. 2014). Much attention has been given to the identification of past and potential future trends in drought events; this has also been the subject of some debate. For example, reports of increases in the severity and/or magnitude of droughts in recent decades (e.g., Dai 2013) have been questioned by others (e.g., Seneviratne 2012; Sheffield et al. 2012a). Despite the uncertainty over recent trends, it seems accepted widely that with a more intense hydrological cycle under climate change (Held and Soden 2006), increased drought occurrence is probable (Sheffield and Wood 2008), with increased magnitude of drought events particularly in more arid regions such as southern Europe (Orlowsky and Seneviratne 2013).

Given the likelihood of increased drought hazard and the need to mitigate drought impacts, improved understanding

Denotes Open Access content.

Corresponding author address: Daniel Kingston, Department of Geography, University of Otago, P.O. Box 56, Dunedin, 9054 New Zealand.
E-mail: daniel.kingston@otago.ac.nz

DOI: 10.1175/JCLI-D-14-00001.1

of the controls on drought occurrence is vital. Such knowledge is critical to enable improved detection and prediction of drought onset. Previous studies have sought to establish the atmospheric controls on drought occurrence at the European (or sub-European) scale, for both meteorological and streamflow drought indicators. Several researchers have focused on the role of atmospheric circulation patterns, such as the North Atlantic Oscillation (NAO). For example, López-Moreno and Vicente-Serrano (2008) investigated the European scale response of the 12-month standardized precipitation index (SPI) to the NAO and found opposing NAO–SPI relationships between northern and southern Europe (positive relationship in the north; inverse relationship in the south). Similar results were obtained using a regionalized SPI for Europe (Hannaford et al. 2011). Although most studies focus on the role of the NAO during winter, the summer NAO (Folland et al. 2009) has been linked also to European-scale drought variation (Linderholm et al. 2009), defined in this instance using the Palmer drought severity index (PDSI). As with the studies of López-Moreno and Vicente-Serrano (2008) and Hannaford et al. (2011), a dipolar influence of the summer NAO on meteorological drought was found between northern and southern Europe. The NAO was also identified as an important driver of hydrological drought events across Europe by Parry et al. (2012).

The key role of the NAO for drought occurrence is unsurprising given that it is the primary mode of atmospheric circulation in the extratropical Northern Hemisphere, and in particular the North Atlantic region (Barnston and Livezey 1987). However, there remains uncertainty over the connections in the process cascade that link such large-scale climate diagnostics to large-scale atmospheric variation and, in turn, precipitation deficits. For example, although van der Schrier et al. (2006) showed strong regional correlation between the NAO and PDSI across Europe, this correlation did not map clearly onto the leading spatial modes of variability identified in the PDSI. Similarly, Bordi and Sutera (2001) identified one of the leading modes of the Europe-wide 24-month SPI to be similar in spatial pattern to the NAO, but not in terms of time series variation. Complexities in NAO–hydrological drought relationships have also been identified. For example, the event-based analysis of Parry et al. (2012) showed that the 1995–97 European drought was associated with a positive, followed by a negative, NAO state. Furthermore, the 1975/76 event, one of the most severe European droughts on record, was found to have only a weak connection to the NAO (Parry et al. 2012).

In part, the lack of clarity in NAO–drought relationships is linked to the limitations of correlation-based analysis using fixed-point NAO indices, rather than gridded circulation data over the study domain. Although circulation pattern indices are powerful potential descriptors of large-scale climate variation, it is not always straightforward to understand the subtleties of the connection between a circulation index and physical climate dynamics (Kingston et al. 2006). Reflecting this complexity, connections between circulation indices, local climate, hydrological variation (including drought) are often more complex than can be described adequately through index-based approaches—as demonstrated by analyses based on gridded climate fields (e.g., Kingston et al. 2009, 2013; Lavers et al. 2010, 2013; Parry et al. 2012). Furthermore, circulation patterns other than the NAO have been shown to be influential for European-scale drought, notably the Scandinavian (SCAN) and eastern Atlantic/western Russia (EA/WR) patterns (Hannaford et al. 2011; Parry et al. 2012). Indeed, the SCAN pattern has been shown to modulate the characteristic climate signal of the NAO (Comas-Bru and McDermott 2014). Despite their apparent influence on European climate, the role of these other circulation patterns has gained relatively little attention in comparison to the NAO. It may be hypothesized that the influence of other circulation patterns may be a contributing factor to the varied results of previous studies of NAO–European drought relationships.

A further potential source of uncertainty in atmospheric circulation–drought relationships is related to the method used to identify drought. Different drought indices are sensitive to drought development over varying time scales and to drought in different parts of the atmosphere–land surface system (e.g., meteorological, soil moisture, or hydrological drought). For example, the SPI may be calculated at multiple temporal resolutions (i.e., it is multiscalar) and is comparable across different climate zones because it is normalized relative to local climatology. However, it is based on precipitation only and so ignores both the evaporation component of the climatic water balance and terrestrial stores and fluxes. The more recently proposed standardized precipitation evapotranspiration index (SPEI; Vicente-Serrano et al. 2010) is formulated following the same statistical method as the SPI; but it is based on climatic water balance, defined as precipitation minus potential evapotranspiration. Climatic water balance, as defined originally by Thornthwaite (1948), has been used as an index of climate change (Crimmins et al. 2011) and can be used for drought monitoring. By calculating accumulated climatic water balance deficit, the SPEI may provide information on soil moisture and hydrological droughts, too. However, such information remains approximate owing to the reliance on potential evapotranspiration,

which by definition does not account for terrestrial limiting conditions (i.e., available water). Notwithstanding this limitation, the SPEI can be viewed as a pragmatic measure based on the commonly used climate water balance simplification that incorporates the effects of increased air temperature or heat waves, while avoiding the need for extensive soil and land cover data used for the full terrestrial water balance modeling. A third commonly used drought index is the PDSI, which is based on precipitation and potential evaporation in combination with a simplistic soil moisture routine (Palmer 1965). However, a series of problems have been identified with the PDSI associated with its fixed time scale and the difficulty of application across different physiographic environments (Alley 1984; Guttman 1998; Seneviratne 2012). So, while the PDSI and SPEI both add a terrestrial dimension to estimates of water availability, their varying data requirements and underlying assumptions result in different indices. In combination with the sole focus of the SPI on precipitation, it is not surprising that analyses based on these three indices have resulted in varying relationships with atmospheric circulation patterns. Because a comprehensive mathematical definition of drought is impractical (Lloyd-Hughes 2014), it is important to understand what a particular drought index is measuring when attempting to assess links with atmospheric circulation.

Given the above research gaps, there is a clear need for improved understanding of atmospheric circulation drivers of European-scale meteorological drought, and of the sensitivity of such drivers to the way in which drought is characterized. The analyses presented here address this research gap by identifying European-scale droughts and investigating the relationship between drought events and large-scale atmospheric circulation. These aims are achieved as follows: 1) the SPI and SPEI are used to identify precipitation and meteorological droughts, respectively; 2) the correlation of the percent area in drought based on the two drought indices with large-scale atmospheric fields over the whole study period (1958–2001) is investigated; and 3) meteorological variation associated with the onset of individual large-scale drought events is studied. The correlation analysis provides a more detailed evaluation of the processes linking large-scale atmospheric variation to European meteorological drought occurrence than has been presented before. Meanwhile, the event-based approach provides additional information on the causes of initiation of the most widespread European drought events, and the extent to which these vary from the general relationships identified by the first approach. The manuscript is structured as follows: section 2 presents the data and methods used; section 3 the results, which are then discussed in section 4. Section 5 presents the conclusions.

2. Data and methods

a. Data and drought indices

A monthly time series of the percentage area of Europe in drought was developed using the Water and Global Change (WATCH) Forcing Dataset (WFD; Weedon et al. 2010), a bias-corrected version of the 40-yr European Centre for Medium-Range Weather Forecasts (ECMWF) Re-Analysis (ERA-40) dataset covering the period January 1958–December 2001 with a $0.5° \times 0.5°$ grid resolution. The underlying ERA-40 dataset has been used widely for investigating global climatic changes through the twentieth century (e.g., Déry and Wood 2005; Gedney et al. 2006; Simmons et al. 2004). Bias correction of the WFD is based on the University of East Anglia Climatic Research Unit (CRU) global 0.5° monthly time series, version 2.1 (CRU TS 2.1; Mitchell and Jones 2005) and the Global Precipitation Climatology Centre version 4 (GPCC v4; Schneider et al. 2008) observations, with temperature corrections for elevation, monthly average, and diurnal temperature range. Bias correction for precipitation includes number of wet days, gauge catch corrections, monthly totals, and the ratio of rainfall: snowfall. Validation of the WFD with FLUXNET stations (Weedon et al. 2010) shows satisfactory agreement for subdaily variations, but very good agreement with monthly observations for temperature and precipitation. The European domain is defined here as the region between 34°–72°N and 13°W–32°E, resulting in 3950 land grid cells of the University of East Anglia CRU land surface mask.

Drought is defined for each grid cell using the SPI and SPEI normalized for that cell. The SPI, outlined by McKee et al. (1993) and Guttman (1999), measures normalized anomalies in precipitation accumulated over a given number of months. The SPEI (Vicente-Serrano et al. 2010) uses the same technique to describe anomalies, but for the climatic water balance (precipitation minus potential evapotranspiration). The SPI has been recommended by several government organizations as a key drought indicator (World Meteorological Organization 2006; Hayes et al. 2011) to examine historical characteristics of drought (Lloyd-Hughes and Saunders 2002), to identify links with atmospheric conditions (Hannaford et al. 2011; Bordi and Sutera 2001), and to monitor progression of drought in real time (Hayes et al. 1999; Quiring 2009). The more recently developed SPEI

(Vicente-Serrano et al. 2010) has yet to be applied widely, but in theory provides a more comprehensive description of water availability than the SPI.

The SPI (SPEI) is computed by summing precipitation (precipitation minus potential evapotranspiration) over k months, termed the accumulation period, and fitting the accumulated values to a parametric statistical distribution from which nonexceedence probabilities may be transformed to the standard normal distribution ($\mu = 0, \sigma = 1$) (Guttman 1999; McKee et al. 1993). Hence, SPI (SPEI) values represent the number of standard deviations from typical accumulated precipitation (climatic water balance) for the location and temporal resolution of calculation (i.e., 0.5° grid cell and monthly resolution in this instance).

The SPI and SPEI datasets were generated following the methodology outlined in Stagge et al. (2014, manuscript submitted to *Int. J. Climatol.*), using a 6-month accumulation period (SPI-6 and SPEI-6) and the recommended two-parameter gamma and generalized extreme value (GEV) distributions to normalize SPI and SPEI values, respectively. Potential evapotranspiration was derived using the Food and Agriculture Organization (FAO-56) Penman–Monteith equation with the Hargraves–Samani simplification for net radiation (Hargreaves and Samani 1985), as described in Allen et al. (1998) and Stagge et al. (2014). Index values were normalized relative to the WMO standard period 1970–99, and limited to the range from −3 to 3 to ensure reasonableness. This range was set one standard deviation beyond the limits of the historical data series, corresponding to a return period of approximately 700 yr, at the far reaches of reasonable extreme hydrological event analyses. A 6-month accumulation period was selected following comparison with other accumulation periods (1, 3, 9, and 12 months). Use of a 6-month period is considered reasonable in terms of physical processes, as it represents a typical seasonal drought within Europe, capturing both ''classical rainfall deficit droughts'' in summer and ''snow-based droughts'' in winter (Van Loon and Van Lanen 2012). In addition, the 6-month accumulation period is well correlated with hydrological droughts in both rapidly recharging headwaters and more hydrologically buffered lowland basins (López-Moreno et al. 2013). Monthly SPI-6 and SPEI-6 values below −0.84 (corresponding to a 20% nonexceedence frequency) were taken as indicative of drought conditions. The 20% nonexceedance level was selected, similar to previous studies (Tallaksen and Stahl 2014; Sheffield et al. 2012b), as a compromise between retaining enough events for a robust analysis and ensuring those events are deemed extreme.

b. Atmospheric circulation–drought analyses

Relationships between atmospheric circulation and the percent area in drought based on SPI-6 and SPEI-6 were explored using correlation analysis. As the SPI-6 and SPEI-6 are based on precipitation and climatic water balance, respectively, accumulated over a 6-month period, these indices were correlated with meteorological fields averaged over the same 6-month accumulation period (e.g., May SPI-6 was correlated with December–May mean climate fields). Meteorological fields chosen as possible drivers of drought were 500- and 1000-hPa geopotential height and wind vector, all sourced from the ERA-40 dataset (following Kingston et al. 2007, 2013).

In addition to the general relationship between the percentage of Europe experiencing climatic water balance drought and atmospheric circulation, individual major widespread drought and their atmospheric drivers were investigated. Unlike correlation analysis, which relates a continuous time series of area in drought and associated meteorological drivers, this analysis focuses on the onset of exceptionally widespread drought events, analyzing only the 6-month period preceding the onset of a small subset of major SPI-6 or SPEI-6 drought events. Here, a major widespread drought event was defined as a multimonth event where >40% of the European land surface area had SPI/SPEI values below −0.84 for at least two consecutive months, or two months where >40% of Europe had SPI/SPEI values below −0.84 separated by no more than one <40% month. Sensitivity to variation (±5%) in the spatial threshold of 40% was investigated; although the number of drought events changed, the atmospheric circulation drivers of drought differed little.

The event-based approach is adopted to permit analysis of the full range of atmospheric conditions leading to the onset of the most extreme drought events in terms of spatial coverage, and to determine the extent to which such conditions vary between events and the more general time series relationships identified by the correlation analysis. Individual extreme events, rather than composites of extreme events, are analyzed as the generation of composites may provide an unrealistic indication of the drivers of meteorological drought given the multiple drivers of European drought identified previously (e.g., Parry et al. 2012). Event-based analysis is a useful approach because it allows for consideration of the location of areas in drought, information that is not considered in the area-based correlation analysis described above. For example, the dominant drivers of drought may vary between different regions of Europe (e.g., Fleig et al. 2011; Kingston et al. 2013). To maintain

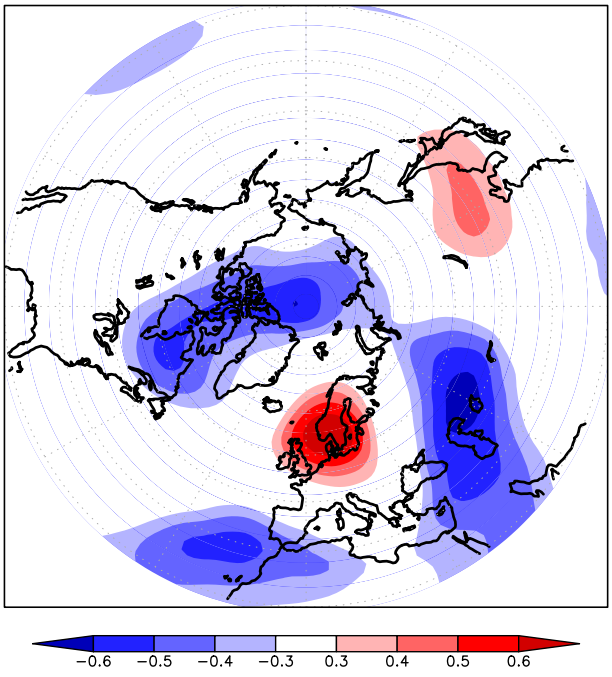

FIG. 1. Correlation of May SPI-6 with December–May mean 500-hPa geopotential height.

consistency with the correlation analysis, the climate conditions are examined for the 6-month period over which the extreme (area in drought >40%) SPI-6 and SPEI-6 drought events are initiated.

3. Results

a. *Correlation with meteorological fields*

Correlation of percent area in drought for both the SPI-6 and SPEI-6 indices with 6-month mean 500-hPa geopotential height and sea level pressure indicates relationships between European drought extent and hemispheric-scale atmospheric circulation. Statistically significant correlation occurs in every month of the year; but correlation is strongest for the SPI-6 and SPEI-6 from March to June. The spatial pattern of correlation is virtually identical for the SPI-6 and SPEI-6, and forms a meridionally orientated dipole over the eastern North Atlantic/western Europe, with positive correlations centered over southern Scandinavia, and negative correlations centered to the southwest of the Iberian Peninsula near the position of the Azores high (exemplified in Fig. 1 for the SPI-6). These results indicate a weaker meridional pressure gradient over western Europe during drought events. This change in circulation is reinforced by the pattern of correlation between the drought indices and the zonal and meridional components of the 500-hPa wind field (Fig. 2), which shows an inverse relationship between the area in drought and the strength of the westerly circulation.

When the pattern of correlation between SPI-6 and SPEI-6 and geopotential height is considered at the hemispheric scale, additional negative correlation centers are apparent over the Caspian/Aral Sea region of Eurasia and the Canadian Arctic (Fig. 1), primarily from March to June. Combined with the pattern of changes in the zonal and meridional components of wind (Fig. 2), these correlation centers suggest a large-scale modification in the nature of hemispheric circulation associated with drought development in Europe.

As an aid to interpretation of the spatial pattern of correlation centers, time series of the SPI-6 and SPEI-6 are correlated with circulation pattern indices whose spatial expression resembles Fig. 2, that is, the NAO, EA/WR, and SCAN (Table 1). Other leading Northern Hemisphere circulation pattern indices (as defined by Barnston and Livezey 1987) were also considered, but with no statistically significant relationships identified. The SPI-6 is correlated moderately with the EA/WR pattern (coefficient of 0.33), and weakly with the NAO and SCAN patterns. The SPEI-6 is correlated moderately with the NAO (0.30), weakly with the EA/WR, but not with the SCAN.

b. *Meteorological control of widespread drought events*

In total, six SPI-6 drought events were identified within the 1958–2001 time period that covered >40% of the European continent for a multimonth period (Fig. 3, Table 2). Notably, four of these events begin in March (i.e., indicating precipitation deficits from October to March). A higher number of widespread multimonth SPEI-6 events occur (i.e., eight; Fig. 3 and Table 2). There are two major SPI-6 drought events that are not SPEI-6 events, whereas there are four SPEI-6 events that are not SPI-6 events. In contrast to the major SPI-6 events, there is little consistency in the month of onset of major SPEI-6 events.

As might be expected for individual observations compared to summary statistics, the atmospheric circulation drivers for individual SPI-6 and SPEI-6 drought events display some variability from the spatial correlation of the drought indices with climate fields (i.e., section 3a; Fig. 1). Specifically, there are two typical patterns of atmospheric circulation anomalies evident in the six months over which the major SPI-6 and SPEI-6 drought events develop. The first pattern (referred to hereafter as the "dipole pattern") comprises a near meridionally orientated dipole of geopotential height anomalies in the mid- to eastern Atlantic, with the positive anomaly center to the north and the negative

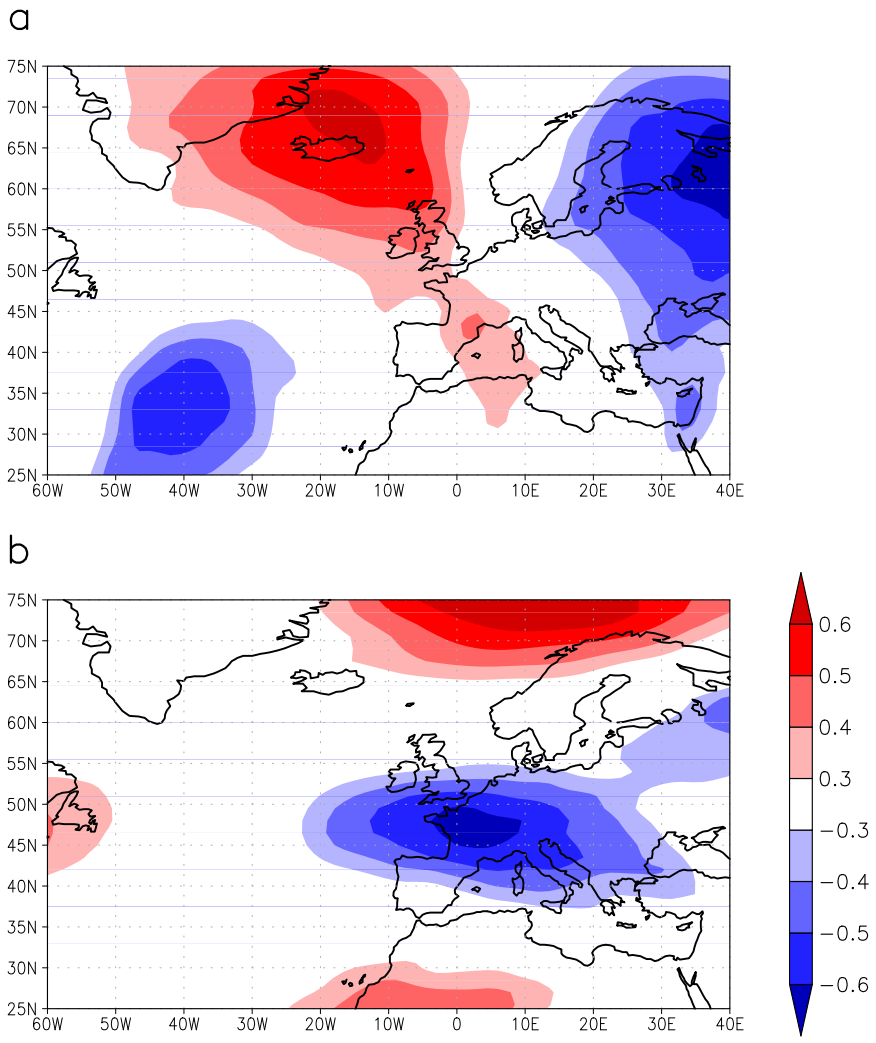

FIG. 2. Correlation of May SPI-6 with December–May mean 500-hPa (a) meridional and (b) zonal wind.

center to the south (as exemplified in Fig. 4a). As such, these anomalies have some similarity to the spatial correlation analysis results (Fig. 1) as they show drought to be associated with a relatively weak geopotential height Atlantic dipole (Fig. 4b) in comparison to the long-term average (Fig. 4c). The 1963, 1964, and 1995/96 droughts can be classified as dipole-driven events (Table 2). The remaining drought events (Table 2) are instead associated with a large positive geopotential height anomaly centered over western Europe (Fig. 5a). The pressure and wind fields associated with this anomaly demonstrate that these changes are associated with an Azores high that extends farther north and east than its climatological average (Figs. 5b,c). As such, this second pattern is referred to hereafter as the "Azores high pattern." In turn, a weaker westerly circulation over Europe (Fig. 5b) compared to the long-term average (Fig. 5c) is observed. Over larger spatial scales, this anomaly sometimes forms part of a wider zonal pattern of positive and negative anomalies across from the Atlantic to Eurasia. In this respect, the Azores high pattern also displays some similarity to the spatial correlation analysis results (Fig. 1).

The two general patterns of geopotential height anomalies described above can be related to different

TABLE 1. Correlation coefficients between the percent area in drought (SPI-6 and SPEI-6) and various circulation pattern indices. Only coefficients significant at $p < 0.05$ are given.

Circulation pattern	SPI-6	SPEI-6
NAO	0.18	0.30
EA/WR	0.33	0.19
SCAN	0.11	—

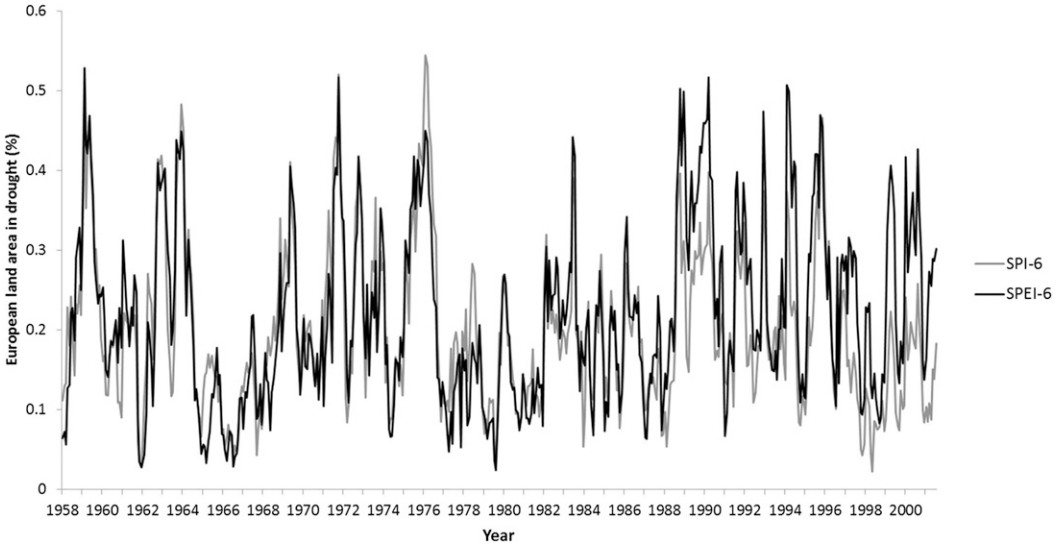

FIG. 3. Time series of the proportion of European land area in drought based on the SPI-6 and SPEI-6 indices.

spatial patterns of drought occurrence. Meridional dipole-driven droughts are associated with drought focused in northern Europe, typically extending from Britain to the eastern limit of Europe (e.g., 1963, Fig. 6a). The spatial pattern of drought associated with the stronger Azores high varies depending on the exact position of the positive height anomaly; but it is typically less focused in northern Europe than dipole-driven droughts and so also includes the Iberian and Mediterranean regions of Europe (e.g., 1976, Fig. 6b). Notably, Azores high–driven Europe-wide droughts comprise the greatest proportion of SPEI-6 drought events, including several events not identified by the SPI (Table 2).

4. Discussion

Overall, the results indicate a series of patterns of large-scale climate variation that are physically consistent with the spatial extent of European drought and with the onset of major European drought events. Considering only the proportion of the European land surface area in drought at any given time (and regardless of the exact location of drought), year-round links to atmospheric circulation occur in the form of centers of correlation in the Canadian Arctic, eastern Atlantic, and Eurasia (Fig. 1). As evidenced by the associated changes in the wind field (Fig. 2), these correlation centers appear physically consistent with the changes in precipitation delivery mechanisms (i.e., reduced incidence of moist maritime Atlantic weather systems) that may be expected to lead to precipitation deficits and excess evaporation.

The spatial pattern of opposing correlation centers from northern Europe into Eurasia (Fig. 1) is similar to the centers of action of the EA/WR atmospheric circulation pattern (Barnston and Livezey 1987). The direction of the

TABLE 2. Timing and driver of major multimonth European SPEI-6 and SPI-6 droughts (where driver is determined by the mean 500-hPa geopotential height field over the 6-month period of drought development).

Timing		
SPEI-6	SPI-6	Driver
July–November 1959	July and September–November 1959	Azores high
—	March–May 1963	Dipole
February–June 1964	March–June 1964	Dipole
—	December–March 1971/72	Azores high
December 1975, February–March and June–August 1976	March–October 1976	Azores high
November–December 1983	—	Azores high
February–June 1989	—	Azores high
March–August 1990	—	Azores high
July–December 1994	—	Azores high
December–January 1995/96 and March–April 1996	March–May 1996	Dipole

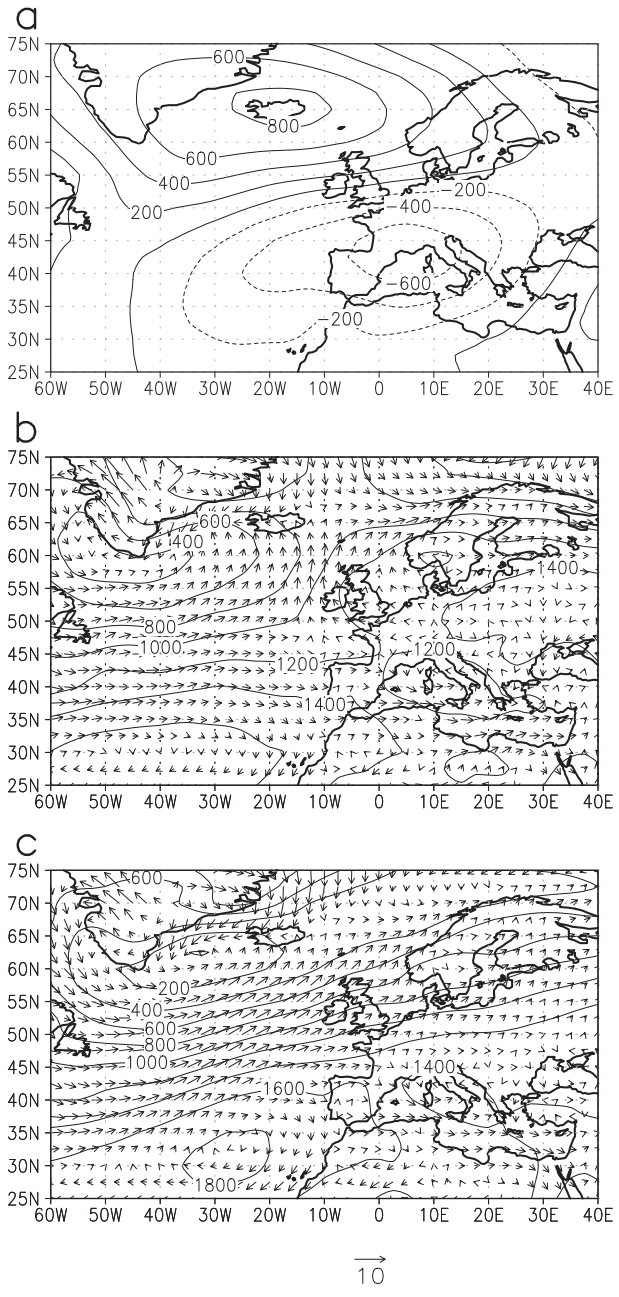

FIG. 4. Exemplar geopotential height and wind fields for dipole-driven drought: (a) October–March 500-hPa geopotential height anomaly for 1962/63, (b) October–March 1000-hPa geopotential height and wind field for 1962/63, and (c) October–March 1958–2001 mean 1000-hPa geopotential height and wind field.

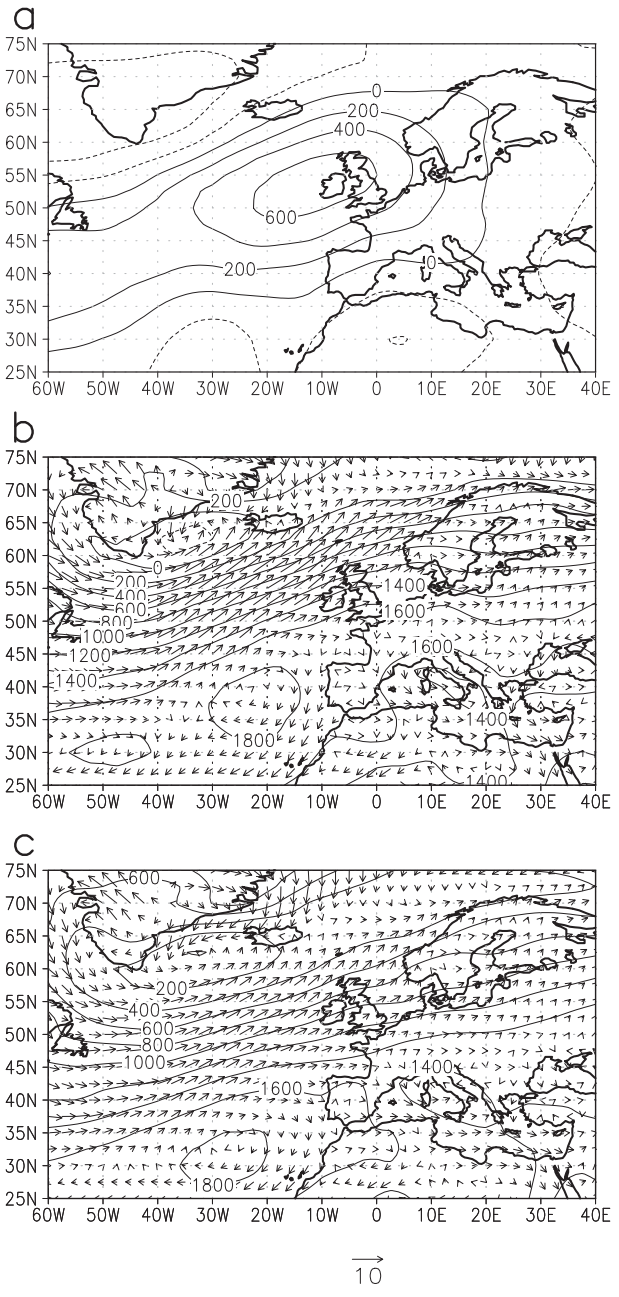

FIG. 5. Exemplar geopotential height and wind fields for Azores high–driven drought: (a) October–March 500-hPa geopotential height anomaly for 1975/76, (b) October–March 1000-hPa geopotential height and wind field for 1975/76, and (c) October–March 1958–2001 mean 1000-hPa geopotential height and wind field.

correlation indicates that a positive EA/WR is associated with drought. The positive phase of this pattern is associated with above-average temperatures and below-average precipitation in western and central Europe, due to a weaker maritime influence on climate—as indicated by Figs. 1 and 2, and previous studies (Krichak and Alpert 2005; Climate Prediction Center 2013). As such, the apparent link to the EA/WR is physically consistent with the development of drought conditions as recorded by the SPI-6 and SPEI-6. Furthermore, previous studies have highlighted the importance of this circulation pattern for European rainfall (Krichak and Alpert 2005) and for individual European drought events (Hannaford et al. 2011; Parry et al. 2012).

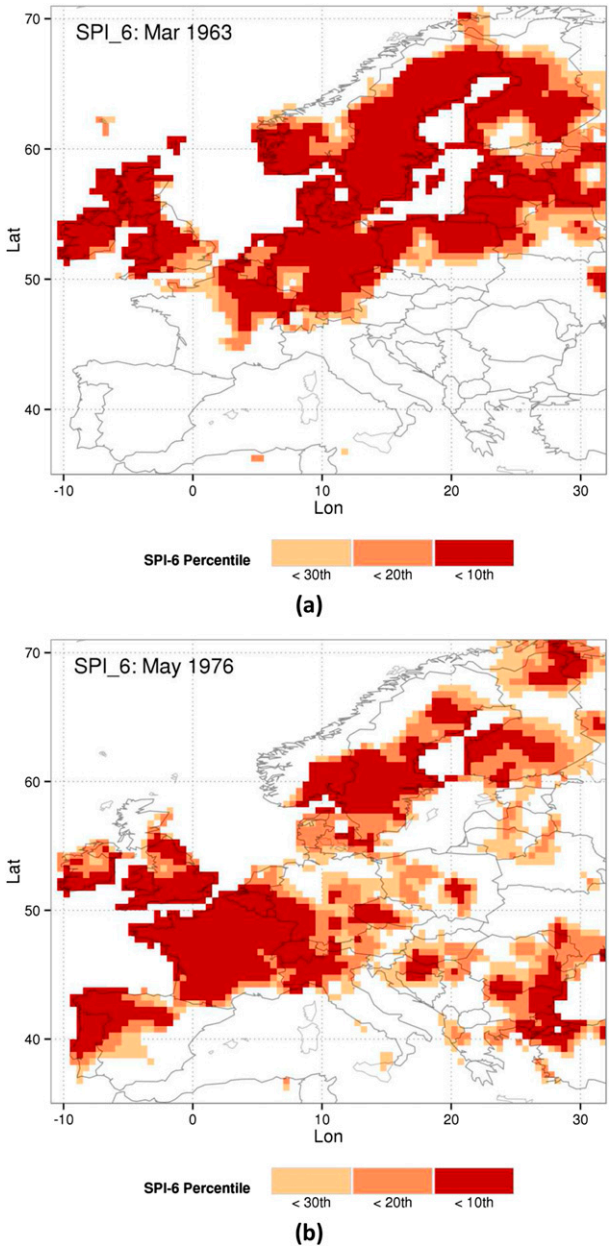

FIG. 6. Exemplar spatial patterns of drought for (a) dipole-driven and (b) Azores high–driven drought.

In addition to the similarity of the correlation pattern in Fig. 1 to the EA/WR signature in geopotential height, the opposing correlation centers between northern Europe and the Azores region strongly suggest the influence of the NAO. The sign of these correlation centers indicate a negative NAO is associated with European drought, which corresponds to the findings of previous studies as discussed in the introduction.

The spatial correlation patterns displayed in Fig. 1 (and so the apparent relationship between drought and the EA/WR and NAO) are strongest from March to June, indicating precipitation or meteorological water balance deficits from October to June. The increased strength of this link during the winter half-year is likely to be associated with the greater spatial coherence in large-scale atmospheric circulation during the winter half-year making large-scale atmospheric circulation patterns generally stronger and easily distinguished at this time of year.

Despite the similarity of the spatial patterns of correlation presented in Figs. 1 and 2 to those associated with the EA/WR and NAO, correlation of the SPI-6 and SPEI-6 time series with the EA/WR and NAO is weak (although statistically significant; Table 1). A possible interpretation of this seeming contradiction is that the principal component analysis (PCA)-based EA/WR and NAO indices are imperfect descriptors of variation in these circulation patterns (as noted previously for the NAO; Kingston et al. 2006), and of relationships between these circulation patterns. For example, according to the PCA definition of these patterns the NAO and EA/WR time series are statistically independent, yet it has also been shown previously that circulation patterns in this region are not independent of each other (Comas-Bru and McDermott 2014). The combination of the EA/WR and NAO (and SCAN for the SPI-6) in a stepwise regression to predict the SPI-6 or SPEI-6 does result in higher predictive power, but the increase in the R^2 value for the resultant multiple regressions is relatively small (from 0.09 to 0.11 for the SPEI-6 and from 0.11 to 0.14 for the SPI-6). The small increase in shared variation further suggests some similarity in terms of drivers of European drought between the three circulation patterns. However, the disparity between the strength of the spatial versus time series correlation statistics remains a matter for further research.

Results from the analysis of meteorological conditions associated with the onset of individual major European drought events permit some distinction to be made between the apparent influence of the EA/WR and NAO circulation patterns on European drought, and in particular drought onset. Specifically, the dipole pattern of geopotential height anomalies associated with drought onset resembles the NAO atmospheric circulation pattern, and the Azores high pattern resembles the spatial signature of EA/WR. As noted in the results, the Azores high pattern is more frequently associated with SPEI-6 drought events. However, Table 1 indicates that the SPEI-6 is better correlated with the NAO in comparison to EA/WR. This apparent contradiction may be because the correlations are based on the entire time series of percent area in drought, while the event-based analysis focuses only on the subset of events with the most spatially extensive drought.

This variation in atmospheric drivers of the onset of individual major drought events, and variation in atmospheric drivers of SPEI-6 versus SPI-6 events, may be explained partially by differences in the drought location and the type of drought that is being measured. For example, it is shown that the dipole pattern (i.e., NAO) is associated primarily with drought conditions in northern Europe, whereas Azores high–driven (i.e., EA/WR) droughts are more variable and widespread in location (Figs. 4–6). This difference in location of drought occurrence is consistent with the climatological implications of a geopotential height dipole such as that in Fig. 4, which would be expected to result in opposing precipitation anomalies over northern and southern Europe (e.g., Lavers et al. 2013).

In addition to spatial variation in the impacts of specific circulation patterns, there are different climatic causes of drought onset such as rainfall deficits and high evapotranspiration losses, which can help to explain the difference in drought forcing patterns between SPI and SPEI events. The choice of drought index defines the type of drought event measured (Lloyd-Hughes 2014); therefore, it follows that the specific atmospheric drivers may differ. Dipole-driven droughts are captured by both the SPI and SPEI, but there are no SPEI-only droughts caused by the dipole pattern. With such a small sample size it is not possible to be definitive, but this result may indicate that dipole (and so SPI) droughts are associated primarily with precipitation deficits rather than excessive evapotranspiration. This is physically consistent given the northern European location of the dipole droughts, the onset of most of these events following water deficits over the winter half-year and the relatively cool and wet climate experienced in this region at this time of year (potential evapotranspiration will be small, similar to actual losses).

Given the different immediate causes of drought (i.e., precipitation versus climatic water balance deficit), the SPEI is likely to be preferable to the SPI as a meteorological drought indicator in southern Europe or in locations where abnormally high evapotranspiration may drive soil moisture or hydrological droughts. The inclusion of 1990 and 1994 as drought events by the SPEI and not the SPI highlights the improved climatic water deficit detection capability of the SPEI in southern Europe, as the period between 1990 and 1995 is considered one of the driest in the century for the Iberian Peninsula (Sheffield et al. 2012a) and produced severe drought impacts across the Mediterranean region (Llamas 2000). Despite this capability, because of the SPEI's dependence on potential evapotranspiration it should always be viewed as a measure of accumulated climatic water balance which only approximates the true terrestrial water balance. In contrast, both indices (SPI and SPEI) are equally effective in identifying climatic water deficits (and so drought) in the cooler northern regions of Europe.

5. Conclusions

This study has presented two time series of European drought extent based on two meteorological drought indices: the SPI and SPEI. A series of physically consistent atmospheric circulation controls on drought events at the European spatial scale has also been revealed. A combination of the NAO and EA/WR circulation patterns are found to be the most important drivers of the proportion of European land area experiencing drought on a monthly time scale.

Controls on the onset of individual drought events vary according to the location of drought within Europe, emphasizing the importance of the additional information provided by the event-based approach. Notably, the most widespread multimonth drought events fall relatively neatly into two categories in terms of spatial extent and atmospheric circulation drivers. Typically, the onset of major droughts centered in northern Europe is associated with an Atlantic meridional dipole circulation anomaly resembling the NAO. Initiation of major droughts that are centered elsewhere in Europe are associated primarily by a northeastward expansion of the Azores high and associated anomalies that resemble the EA/WR. Thus, the more varied relationships associated with onset of individual major events (cf. the overall drought-area time series) reflect the variability in climate situations that can cause drought in different parts of Europe. As a result of the apparent dual causes of major drought development, creating a uniform composite of drivers of drought is challenging. Similarly, this duality offers an explanation as to the relative absence of straightforward linear relationships between atmospheric circulation pattern indices and drought indices in previous studies. Despite the complexity shown here in the process cascade from large-scale climate to European-wide drought, these analyses provide new information on the climatic processes associated with the occurrence of different types of meteorological drought (precipitation and climatic water balance deficit) across the range of European climate regions, and so provide vital context for ongoing studies of the predictability of European drought.

Acknowledgments. This work was supported by the EU FP-7 Project DROUGHT-R&SPI (Contract 282769), and forms a contribution to the UNESCO-IHP FRIEND-Water Programme. Comments and suggestions from two anonymous reviewers are gratefully acknowledged.

REFERENCES

Allen, R., L. Pereira, D. Raes, and M. Smith, 1998: Crop evapotranspiration. FAO irrigation and drainage paper, Paper 56, FAO, Rome, Italy, 10 pp.

Alley, W. M., 1984: The Palmer drought severity index: Limitations and assumptions. *J. Climate Appl. Meteor.,* **23,** 1100–1109, doi:10.1175/1520-0450(1984)023<1100:TPDSIL>2.0.CO;2.

Barnston, A. G., and R. E. Livezey, 1987: Classification, seasonality and persistence of low-frequency atmospheric circulation patterns. *Mon. Wea. Rev.,* **115,** 1083–1126, doi:10.1175/1520-0493(1987)115<1083:CSAPOL>2.0.CO;2.

Bordi, I., and A. Sutera, 2001: Fifty years of precipitation: Some spatially remote teleconnnections. *Water Resour. Manage.,* **15,** 247–280, doi:10.1023/A:1013353822381.

Climate Prediction Center, cited 2013: Northern Hemisphere teleconnection patterns. National Oceanic and Atmospheric Administration/National Weather Service. [Available online at http://www.cpc.ncep.noaa.gov/data/teledoc/telecontents.shtml.]

Comas-Bru, L., and F. McDermott, 2014: Impacts of the EA and SCA patterns on the European twentieth century NAO–winter climate relationship. *Quart. J. Roy. Meteor. Soc.,* **140,** 354–363, doi:10.1002/qj.2158.

Crimmins, S. M., S. Z. Dobrowski, J. A. Greenberg, J. T. Abatzoglou, and A. R. Mynsberge, 2011: Changes in climatic water balance drive downhill shifts in plant species' optimum elevations. *Science,* **331,** 324–327, doi:10.1126/science.1199040.

Dai, A., 2013: Increasing drought under global warming in observations and models. *Nat. Climate Change,* **3,** 52–58, doi:10.1038/nclimate1633.

Déry, S. J., and E. F. Wood, 2005: Observed twentieth century land surface air temperature and precipitation covariability. *Geophys. Res. Lett.,* **32,** L21414, doi:10.1029/2005GL024234.

Fleig, A. K., L. M. Tallaksen, H. Hisdal, and D. M. Hannah, 2011: Regional hydrological drought in north-western Europe: Linking a new regional drought area index with weather types. *Hydrol. Processes,* **25,** 1163–1179, doi:10.1002/hyp.7644.

Folland, C. K., J. Knight, H. W. Linderholm, D. Fereday, S. Ineson, and J. W. Hurrell, 2009: The summer North Atlantic Oscillation: Past, present, and future. *J. Climate,* **22,** 1082–1103, doi:10.1175/2008JCLI2459.1.

Gedney, N., P. M. Cox, R. A. Betts, O. Boucher, C. Huntingford, and P. A. Stott, 2006: Detection of a direct carbon dioxide effect in continental river runoff records. *Nature,* **439,** 835–838, doi:10.1038/nature04504.

Guttman, N. B., 1998: Comparing the Palmer Drought Index and the Standardized Precipitation Index. *J. Amer. Water Resour. Assoc.,* **34,** 113–121, doi:10.1111/j.1752-1688.1998.tb05964.x.

——, 1999: Accepting the Standardized Precipitation Index: A calculation algorithm. *J. Amer. Water Resour. Assoc.,* **35,** 311–322, doi:10.1111/j.1752-1688.1999.tb03592.x.

Hannaford, J., B. Lloyd-Hughes, C. Keef, S. Parry, and C. Prudhomme, 2011: Examining the large-scale spatial coherence of European drought using regional indicators of precipitation and streamflow deficit. *Hydrol. Processes,* **25,** 1146–1162, doi:10.1002/hyp.7725.

Hargreaves, G. H., and Z. A. Samani, 1985: Reference crop evapotranspiration from ambient air temperature. American Society of Agricultural Engineers Paper 85-2517, 12 pp. [Available online at http://www.zohrabsamani.com/papers/Hargreaves_Samani_85.pdf.]

Haslinger, K., D. Koffler, W. Schöner, and G. Laaha, 2014: Exploring the link between meteorological drought and streamflow: Effects of climate-catchment interaction. *Water Resour. Res.,* **50,** 2468–2487, doi:10.1002/2013WR015051.

Hayes, M. J., M. D. Svoboda, D. A. Wilhite, and O. V. Vanyarkho, 1999: Monitoring the 1996 drought using the Standardized Precipitation Index. *Bull. Amer. Meteor. Soc.,* **80,** 429–438, doi:10.1175/1520-0477(1999)080<0429:MTDUTS>2.0.CO;2.

——, ——, N. Wall, and M. Widhalm, 2011: The Lincoln declaration on drought indices: Universal meteorological drought index recommended. *Bull. Amer. Meteor. Soc.,* **92,** 485–488, doi:10.1175/2010BAMS3103.1.

Held, I. M., and B. J. Soden, 2006: Robust responses of the hydrological cycle to global warming. *J. Climate,* **19,** 5686–5699, doi:10.1175/JCLI3990.1.

Ji, L., and A. J. Peters, 2003: Assessing vegetation response to drought in the northern Great Plains using vegetation and drought indices. *Remote Sens. Environ.,* **87,** 85–98, doi:10.1016/S0034-4257(03)00174-3.

Kingston, D. G., D. M. Lawler, and G. R. McGregor, 2006: Linkages between atmospheric circulation, climate and streamflow in the northern North Atlantic: Research prospects. *Prog. Phys. Geogr.,* **30,** 143–174, doi:10.1191/0309133306pp471ra.

——, G. R. McGregor, D. M. Hannah, and D. M. Lawler, 2007: Climatic controls on New England streamflow. *J. Hydrometeor.,* **8,** 367–379, doi:10.1175/JHM584.1.

——, D. M. Hannah, D. M. Lawler, and G. R. McGregor, 2009: Climate–river flow relationships across montane and lowland environments in northern Europe. *Hydrol. Processes,* **23,** 985–996, doi:10.1002/hyp.7202.

——, A. K. Fleig, L. M. Tallaksen, and D. M. Hannah, 2013: Ocean–atmosphere forcing of summer streamflow drought in Great Britain. *J. Hydrometeor.,* **14,** 331–344, doi:10.1175/JHM-D-11-0100.1.

Krichak, S. O., and P. Alpert, 2005: Decadal trends in the east Atlantic–west Russia pattern and Mediterranean precipitation. *Int. J. Climatol.,* **25,** 183–192, doi:10.1002/joc.1124.

Lavers, D., C. Prudhomme, and D. M. Hannah, 2010: Large-scale climate, precipitation and British river flows: Identifying hydroclimatological connections and dynamics. *J. Hydrol.,* **395,** 242–255, doi:10.1016/j.jhydrol.2010.10.036.

——, ——, and ——, 2013: European precipitation connections with large-scale mean sea level pressure (MSLP) fields. *Hydrol. Sci. J.,* **58,** 310–327, doi:10.1080/02626667.2012.754545.

Linderholm, H. W., C. K. Folland, and A. Walther, 2009: A multicentury perspective of the summer North Atlantic Oscillation (SNAO) and drought in the eastern Atlantic Region. *J. Quat. Sci.,* **24,** 415–425, doi:10.1002/jqs.1261.

Llamas, M. R., 2000. Some lessons learnt during the drought of 1991–1995 in Spain. *Drought and Drought Mitigation in Europe: Advances in Natural and Technological Hazards Research,* J. Vogt and F. Somma, Eds., Springer, 253–264.

Lloyd-Hughes, B., 2014: The impracticality of a universal drought definition. *Theor. Appl. Climatol.,* **117,** 607–611, doi:10.1007/s00704-013-1025-7.

——, and M. A. Saunders, 2002: A drought climatology for Europe. *Int. J. Climatol.,* **22,** 1571–1592, doi:10.1002/joc.846.

López-Moreno, J. I., and S. M. Vicente-Serrano, 2008: Positive and negative phases of the wintertime North Atlantic Oscillation and drought occurrence over Europe: A multitemporal-scale approach. *J. Climate,* **21,** 1220–1243, doi:10.1175/2007JCLI1739.1.

——, ——, J. Zabalza, S. Beguería, J. Lorenzo-Lacruz, C. Azorin-Molina, and E. Morán-Tejeda, 2013: Hydrological response to climate

variability at different time scales: A study in the Ebro basin. *J. Hydrol.,* **477,** 175–188, doi:10.1016/j.jhydrol.2012.11.028.

McKee, T. B., N. J. Doesken, and J. Kleist, 1993: The relationship of drought frequency and duration to time scales. *Proc. Eighth Conf. on Applied Climatology,* Anaheim, CA, Southwest Climate Change Network, 179–183. [Available online at http://ccc.atmos.colostate.edu/relationshipofdroughtfrequency.pdf.]

Mitchell, T. D., and P. D. Jones, 2005: An improved method of constructing a database of monthly climate observations and associated high-resolution grids. *Int. J. Climatol.,* **25,** 693–712, doi:10.1002/joc.1181.

Monk, W. A., P. J. Wood, D. M. Hannah, and D. A. Wilson, 2008: Macroinvertebrate community response to inter-annual and regional river flow regime dynamics. *River Res. Appl.,* **24,** 988–1001, doi:10.1002/rra.1120.

Orlowsky, B., and S. I. Seneviratne, 2013: Elusive drought: Uncertainty in observed trends and short- and long-term CMIP5 projections. *Hydrol. Earth Syst. Sci.,* **17,** 1765–1781, doi:10.5194/hess-17-1765-2013.

Palmer, W. C., 1965: Meteorological drought. Research Paper 45. U.S. Weather Bureau, Washington, DC, 58 pp.

Parry, S., J. Hannaford, B. Lloyd-Hughes, and C. Prudhomme, 2012: Multi-year droughts in Europe: Analysis of development and causes. *Hydrol. Res.,* **43,** 689–706, doi:10.2166/nh.2012.024.

Quiring, S. M., 2009: Monitoring drought: An evaluation of meteorological drought indices. *Geogr. Compass,* **3,** 64–88, doi:10.1111/j.1749-8198.2008.00207.x.

Schneider, U., T. Fuchs, A. Meyer-Christoffer, and B. Rudolf, 2008: Global precipitation analysis products of the GPCC. Global Precipitation Climatology Centre (GPCC), DWD, 12 pp.

Seneviratne, S. I., 2012: Historical drought trends revisited. *Nature,* **491,** 338–339, doi:10.1038/491338a.

Sheffield, J., and E. F. Wood, 2008: Projected changes in drought occurrence under future global warming from multi-model, multi-scenario, IPCC AR4 simulations. *Climate Dyn.,* **31,** 79–105, doi:10.1007/s00382-007-0340-z.

——, ——, and M. L. Roderick, 2012a: Little change in global drought over the past 60 years. *Nature,* **491,** 435–438, doi:10.1038/nature11575.

——, B. Livneh, and E. F. Wood, 2012b: Representation of terrestrial hydrology and large-scale drought of the continental United States from the North American Regional Reanalysis. *J. Hydrometeor.,* **13,** 856–876, doi:10.1175/JHM-D-11-065.1.

Simmons, A. J., and Coauthors, 2004: Comparison of trends and low-frequency variability in CRU, ERA-40, and NCEP/NCAR analyses of surface air temperature. *J. Geophys. Res.,* **109,** D24115, doi:10.1029/2004JD005306.

Stagge, J. H., L. M. Tallaksen, C. Y. Xu, and H. A. J. van Lanen, 2014: Standardized precipitation-evapotranspiration index (SPEI): Sensitivity to potential evapotranspiration model and parameters. *Proc. FRIEND-Water 2014: Hydrology in a Changing World: Environmental and Human Dimensions,* IAHS Publ. 363, Montpellier, France, Institut Montpelliérain de l'Eau et de l'Environnement, 367–373.

Tallaksen, L. M., and H. A. J. van Lanen, Eds., 2004: *Hydrological Drought: Processes and Estimation Methods for Streamflow and Groundwater*. Developments in Water Sciences Series, Vol. 48, Elsevier, 580 pp.

——, and K. Stahl, 2014: Spatial and temporal patterns of large-scale droughts in Europe: Model dispersion and performance. *Geophys. Res. Lett.,* **41,** 429–434, doi:10.1002/2013GL058573.

Thornthwaite, C. W., 1948: An approach toward a rational classification of climate. *Geogr. Rev.,* **38,** 55–94, doi:10.2307/210739.

Tsakiris, G., H. Vangelis, and D. Tigkas, 2010: Drought impacts on yield potential in rainfed agriculture. *Economics of Drought and Drought Preparedness in a Climate Change Context,* A. López-Francos and A. López-Francos, Eds., CIHEAM/FAO/ICARDA/GDAR/CEIGRAM/MARM, 192–197.

van der Schrier, G., K. R. Briffa, P. D. Jones, and T. J. Osborn, 2006: Summer moisture variability across Europe. *J. Climate,* **19,** 2818–2834, doi:10.1175/JCLI3734.1.

Van Loon, A. F., and H. A. J. Van Lanen, 2012: A process-based typology of hydrological drought. *Hydrol. Earth Syst. Sci.,* **16,** 1915–1946, doi:10.5194/hess-16-1915-2012.

Vicente-Serrano, S. M., S. Beguería, and J. I. López-Moreno, 2010: A multiscalar drought index sensitive to global warming: The standardized precipitation evapotranspiration index. *J. Climate,* **23,** 1696–1718, doi:10.1175/2009JCLI2909.1.

——, and Coauthors, 2012: Performance of drought indices for ecological, agricultural and hydrological applications. *Earth Interact.,* **16,** doi:10.1175/2012EI000434.1.

Weedon, G. P., S. Gomes, P. Viterbo, H. Österle, J. C. Adam, N. Bellouin, O. Boucher, and M. Best, 2010: The WATCH forcing data 1958-2001: A meteorological forcing dataset for land surface and hydrological models. WATCH Tech. Rep. 22, 42 pp. [Available online at http://www.eu-watch.org/media/default.aspx/emma/org/10376311/WATCH+Technical+Report+Number+22+The+WATCH+forcing+data+1958-2001+A+meteorological+forcing+dataset+for+land+surface-+and+hydrological-models.pdf.]

WMO, 2006: Drought monitoring and early warning: Concepts, progress and future challenges. World Meteorological Organization Rep. WMO-1006, 24 pp. [Available online at http://www.wamis.org/agm/pubs/brochures/WMO1006e.pdf.]